

Original Article

Finite Element Validation of Theoretical HRR Solution For Mode I Crack Tip Stress Field In EPFM

Sunil Bhat¹, Yashpal Khedkar², C. Solaimuthu³

¹Department of Mechanical Engineering, RVITM, Bangalore, Karnataka, India.

²Department of Mechanical Engineering, SVRI's College of Engineering, Pandharpur, Maharashtra, India.

³Department of Mechanical Engineering, RVITM, Bangalore, Karnataka, India.

²Corresponding Author : ymkhedkar@gmail.com

Received: 09 September 2025

Revised: 10 October 2025

Accepted: 11 November 2025

Published: 28 November 2025

Abstract - Stress field near and in front of the tip of a crack in EPFM regime is governed by energy release rate parameter, “J integral”, which is the plastic analogue of stress intensity parameter “K” commonly employed in LEFM and SSY regimes that are characterized by minimal crack tip plasticity. The available theoretical Hutchinson, Rice, and Rosengren (HRR) solution of the crack tip stress field in EPFM necessitates the use of J in the formulations. This paper presents a finite element analysis of a mode I cracked ductile steel plate under EPFM conditions for obtaining the value of J integral and the stress values in a relatively large crack tip plastic zone, the case falling within the purview of EPFM. Work hardening coefficient and other material constants of steel are determined from the Ramberg-Osgood relation. EPFM condition at the crack tip is numerically simulated by using ANSYS 12.0 software. J integral is obtained over various cyclic nodal paths near and around the crack tip in the post-processor finite element solution. The mean value of J is used in the HRR radial stress solution at a particular node having distinct radial and angular coordinates. The same exercise is repeated for several nodes in the plastic zone. Finite element values of radial stresses at selected nodes are compared with those obtained from the HRR solution. The results nearly match each other, thereby validating the HRR solution.

Keywords - Elastic Plastic Fracture Mechanics, Finite Element Modeling, HRR solution, J integral.

1. Introduction

Ductile materials undergo extensive yielding or plastic deformation when subjected to load. Therefore, the fracture initiated by a crack in such materials is always preceded by large and noticeable yielding at the crack tip, which assumes an important role in the fracture process (Anderson, 2005). Principles of Linear Elastic Fracture Mechanics (LEFM) are essentially meant for cracks in brittle materials that undergo nil plastic deformation. However, LEFM can also be applied with approximations to cracks in ductile materials, provided the yielding near the tip of the crack is of Small Scale (SSY) in comparison with the parent crack size. But for a greater extent of plasticity at the crack tip (nearly of the order of crack size), principles of LEFM and SSY fail to define the crack tip characteristics (Hutchinson 1968), and as a result, the case falls under the purview of Elastic Plastic Fracture Mechanics (EPFM). No K-dominated zone exists in EPFM, and only the J integral holds good. Finally, there is a nil parameter characterization in the case of Large-Scale Yielding (LSY) at the crack tip,

involves the formation of a non-negligible or relatively large yield zone at the tip of the crack. Consequently, the yield zone size and the separate criteria for crack growth constitute two important issues in EPFM.

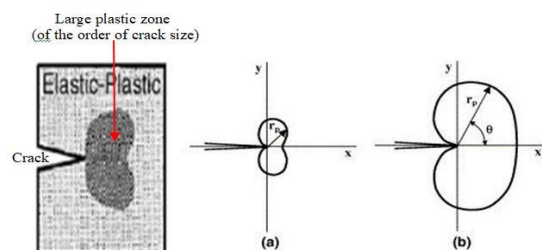


Fig. 1 Schematic of plastic zone at the crack tip in EPFM (a) Plane Strain, and (b) Plane stress conditions (Anderson 2005).

HRR solution, named after Hutchinson, Rice, and Rosengren (1968), presents a theoretical methodology to obtain the magnitude of stress-strain field in the vicinity of a sharp crack tip in a power law material under EPFM conditions. An explicit expression for stress singularity as a function of the power law exponent of the material is also available, but the stress angular variation functions are not in a closed form.

Refer to Figure 1, the EPFM regime is therefore related to non-linear ductile fracture, i.e., when the fracture process



1.1. HRR Solution (Anderson 2005)

HRR postulated stress solution in the crack tip plastic or yield zone of power law strain hardening material as follows:-

$$\sigma_{ij} = \sigma_{ys} \left[\frac{EJ}{\alpha \sigma_{ys}^2 I_n r} \right]^{\frac{1}{n+1}} \tilde{\sigma}_{ij}(n, \theta) \quad (1)$$

Well-known Ramberg-Osgood equation for elastic-plastic material is given as:-

$$\frac{E}{\epsilon_{ys}} = \frac{\sigma}{\sigma_{ys}} + \alpha \left[\frac{\sigma}{\sigma_{ys}} \right]^n \quad (2)$$

Equation (2) enables us to find the values of constants n and α by using the known non-linear stress-strain data (σ , ϵ) of the material. Figure 2 (Anderson 2005) presents the plots of I_n vs n in cases of plane stress and plane strain. Figure 3 provides the value of the angular variation of $\tilde{\sigma}_{ij}(n, \theta)$ for different values of n and θ in the plane stress case.

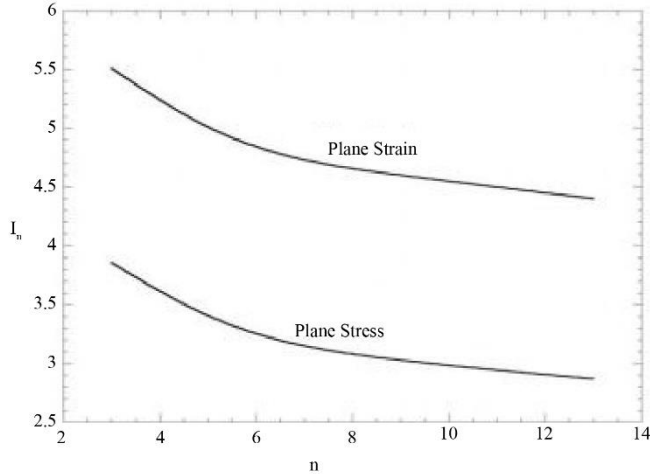


Fig. 2 Effect of strain hardening exponent, n , on HRR integration constant (Anderson 2005)

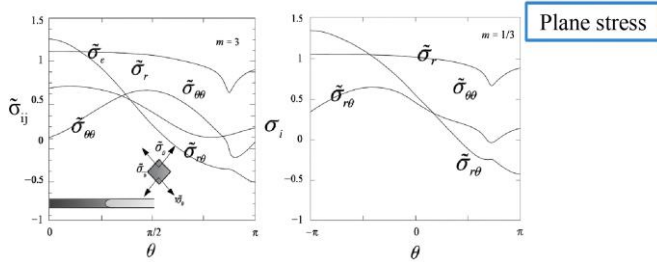


Fig. 3 Angular variation of $\tilde{\sigma}_{ij}(n, \theta)$ for $n=3$ and $n=13$ in plane stress case (Anderson 2005)

1.2. J Integral

J integral, used in Equation (1), is represented in the form of a line integral. Hutchinson, Rice, and Rosengren proved that J precisely models stresses and strains near the crack tip in non-linear materials. Rice (1968) demonstrated that the J

integral is path independent. Refer to Figure 4. The two-dimensional representation of this integral over a cyclic path, Γ , is as follows:-

$$J = \oint \left(w dy - T_i \frac{\partial u_i}{\partial x} ds \right) \quad (3)$$

Density of strain energy, w , is given by $w = \int_0^{\epsilon_{ij}} \sigma_{ij} d\epsilon_{ij}$ where ϵ_{ij} and σ_{ij} are the strain and stress tensors, respectively. Traction vector is defined by $T_i = \sigma_{ij} n_j$, where n_j represents the components of the unit vector normal to the path, Γ .

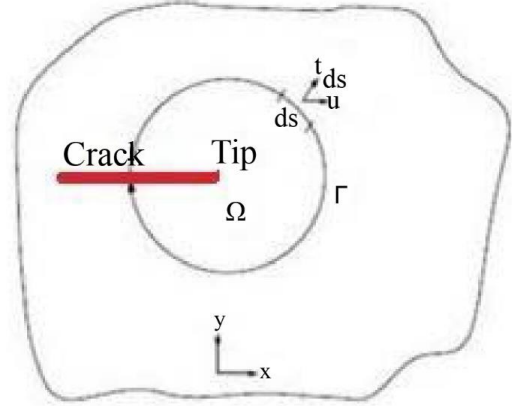


Fig. 4 J integral definition around crack tip (Anderson 2005)

2. Literature Review

Fillipi, Ciavarella, and Lazzarin (2002) developed a theoretical approach for HRR solution of sharp V notches with suitable notch angles under different, i.e., Mode I and II loading conditions. But when the notch opening angle approached zero, the notch assumed the form of a crack, leading to the complicated solution.

Zhao, Guo, and She (2008) presented a three-dimensional, elastic-plastic, finite element analysis of semi-elliptical surface cracks in a plate under far-field tensile force. Elguedj, Gravouil, and Combescure (2006) suggested the application of HRR fields to find the singularities in EPFM. Fourier analysis was undertaken in the process.

Mahyar S. et al. (1990) conducted experimental work by employing moire interferometry to obtain vertical and horizontal displacements for stable crack growth in uniaxially loaded specimens under elastic-plastic conditions. Jingxia Yue et al. (2002) used the energy method to examine the elastic-plastic field of a tensile crack. Chiang et al. (1988) focused on the experimental displacements near a plastically deformed crack tip in different work-hardening materials using HRR field solutions and the optical in-plane and out-of-plane moire method.

Weichen et al. (2010) found the distribution of damage and the generation of the HRR field by means of a two-scalar

damage variable. Sotiropoulou et al. (2006) restored the available approximate asymptotic solutions concerning the HRR field for plane strain conditions in non-linear elastic fracture. Graba (2012) presented the values of Q factor for elastic plastic material in the case of the centre cracked plate in tension and checked the effect of yield strength, work hardening exponent, and crack length on Q factor.

Wang and Chow (1992) investigated the interaction between the crack and distributed damage in an elastic-plastic material based on the HRR model. May and Kobayashi (1995) used moiré interferometry to obtain orthogonal displacements in zones surrounding a stably extending crack in a ductile body.

Of late, Wang et al. (2023) proposed the analytical equation for the equivalent stress of a representative volume element with the median energy density of a finite dimension specimen. Their work was based on energy density equivalence and dimensional analysis. Xu et al. (2025) used the HRR stress-strain field at the crack tip to frame a model that adopted a new size parameter to characterize the size of the cyclic plastic zone at the crack tip.

Nieva et al. (2026) came out with a comprehensive review of published analytical results for solutions under both elastic and elasto-plastic material behaviour regimes, including Williams and HRR solutions. The solutions are compared with results obtained from the 3D finite element discretization. Yue et al. (2022) proposed a delta-CTOD model based on HRR solution while considering the crack closure effect. They also suggested that the HRR model showed better accuracy.

Coming to the problem at hand, Xu, Liu, and Yuan (2022) found that the stress field at the crack tip in the fatigue regime conformed to the results of the available HRR solution. Likewise, Malone, Plunkett, and P. G. Hodge Jr. (1986) compared the numerical and theoretical HRR solution in the SSY regime.

Kikuchi (1992) investigated surface-cracked specimens. Stress and displacement fields at the crack tip were compared with the HRR solution. From the literature review, it is found that there exists the scope to validate the HRR solution in a full-fledged, 2D case, EPFM regime for a through, body crack under monotonic load.

This paper is another step forward in the direction of numerical authentication of available HRR solutions from the basic principles. Also, unlike in the previous work, where nodes on the crack axis in the plastic zone are usually considered for stress measurement and analysis, this work permits picking up of arbitrary nodes anywhere in the plastic zone to verify the spatial effects of the HRR solution as well.

3. Methodology

The undermentioned methodology is adopted in the present work:-

- Finite Element (FE) modeling of Mode I, through, edge crack in a ductile plate is undertaken in Ansys 12.0 software. Suitable plate dimensions (small thickness for the plane stress case) and material properties are used. Non-linear, stress-strain data of the material in Equation (2) are used to obtain the values of n and α .
- The size of the crack and the magnitude of load are fixed in such a manner that the size of the plastic zone at the crack tip is large enough and is of the order of the crack size. This ensures the existence of the EPFM regime.
- Using the post-processor finite element solution, several cyclic nodal paths are manually defined ahead of the crack tip. J integral is found for each path with the help of a computer code that is based on Equation (3). The code is presented in Appendix 1. It is input into the post-processor solution in order to obtain the value of J . The Mean of J over all different paths leads to the final value of J .
- The final value of J integral is used in Equation (1) of HRR formulation to theoretically determine the radial stresses at selected nodes in the plastic zone. Value of I_n for the known value of n is picked from Figure 2. Value of $\bar{\sigma}_{ij}(n, \theta)$ corresponding to the known values of n and θ for radial stress at each chosen node is read from Figure 3. The process is repeated at all the chosen nodes.
- The magnitudes of radial stresses at the selected nodes are finally noted from the post-processor finite element solution, which are then compared with the values obtained from the theoretical HRR solution for validation.

4. Material, Crack, and Load Data

The material considered for computational purposes is ductile, austenitic, stainless steel. The data on stress vs strain of the steel are available in Figure 5.

a) Material properties of the steel are as follows:-

Type/Grade: 301 (S30100) steel

Young's Modulus (E) = 2×10^5 MPa; Yield Strength (σ_{YS}) = 455 MPa; Ultimate Tensile Strength (σ_{UTS}) = 700 MPa; % elongation at σ_{UTS} = 40

From Equation (2), the dimensionless constant, $\alpha = 27.695$, and work hardening coefficient, $n = 4.09$, are obtained.

b) Plate dimensions (Refer to Figure 6 and Figure 7)

Width of the plate, $w = 300$ mm; Height of the plate, $h = 1000$ mm; Thickness-small (2D plane stress case)

c) Mode of fracture, type and size of crack, and far-field applied stress

Opening mode (Mode I) type of crack; Length of the crack, $a = 20$ mm; The crack is through, sharp, and edge type; Value of the applied or far field stress, $p = 300$ MPa

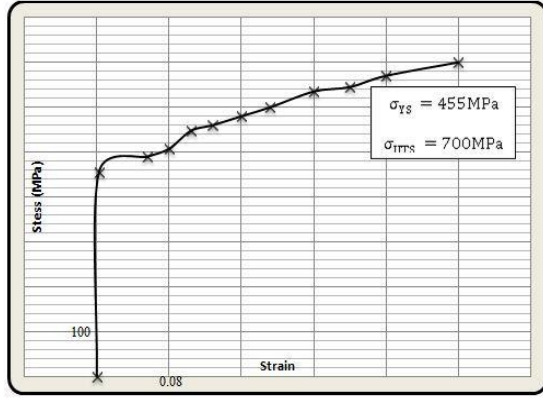


Fig. 5 Stress-strain curve for S30100 grade steel

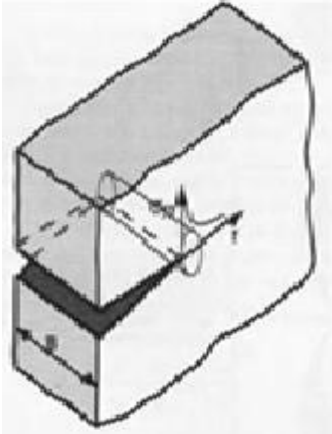


Fig. 6 Mode I (opening mode) of edge crack in a large plate (3D view)

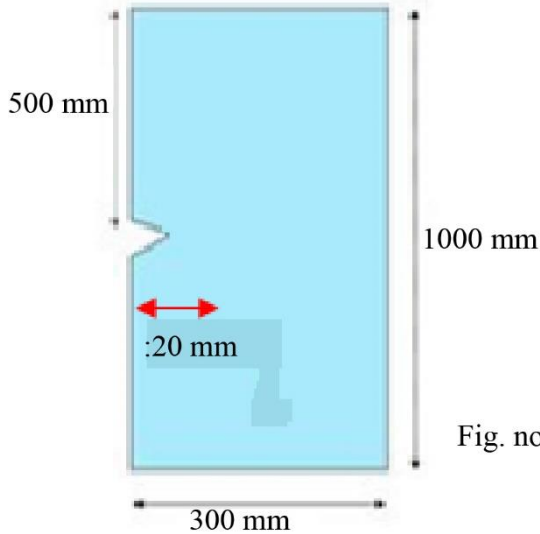


Fig. 7. Mode I (opening mode) of edge crack in a large plate (front view)

5. Finite Element Analysis

Finite Element Analysis (FEA) is undertaken over the cracked plate. Only half of the Mode I plate is modeled, because of the condition of symmetry, in the Ansys 12.0 software. Data pertaining to stress-strain properties of steel in

Figure 5 are used to define the non-linear material model in the software. Refer to Figure 8 for the mesh model of the half plate. Ultra-fine mesh is adopted around the vicinity of the crack tip to enable h-mesh refinement for quick optimization and convergence. Details of nodes and elements are as follows:-

Type of element used: Higher order, 8-node 82

Number of nodes: 338818, Number of elements: 112375

Far field stress equal to 300 MPa is generated in the y direction, perpendicular to the crack, at the top nodes of the model. The nodes at the crack are left unconstrained. All the nodes after the crack tip up to the end of the plate are constrained in the y direction, i.e., $v = 0$. Due to the presence of higher-order elements (p-refinement) and ultra-fine mesh (h-refinement) near the crack tip, the convergence of the solution is achieved in the first iteration itself. J integral values are found over various cyclic paths near and around the crack tip in the processor solution.

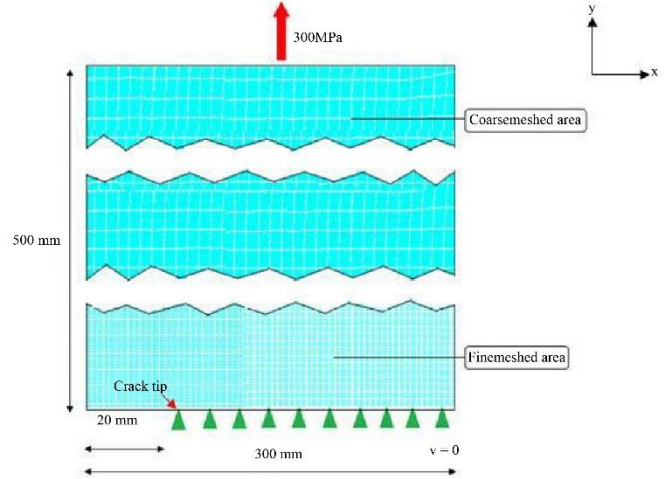


Fig. 8 Mesh model with load and constraints

6. Validation of EPFM

Theoretical estimation of the crack tip plastic zone size in the EPFM regime is quite complex. As an approximation, LEFM principles are extended to the case under consideration for estimation of the yield zone size, r_p , that in the SSY regime is given by Irwin's equation as follows:-

$$r_p = \frac{1}{c\pi} \left[\frac{K_I}{\sigma_{YS}} \right]^2 \quad (4)$$

K_I for Mode I, through, edge crack is equal to $p\sqrt{\pi a} f(\alpha\alpha)$, where $f(\alpha\alpha)$ is a dimensionless crack configuration factor, the magnitude of which is decided by the far field load, crack geometry, and dimensions of the body. $f(\alpha\alpha) = 1.12 - 0.23\alpha\alpha + 10.55\alpha\alpha^2 - 21.27\alpha\alpha^3 + 30.39\alpha\alpha^4$ where $\alpha\alpha = a/w\#$ for $0 < \alpha\alpha < 0.7$. c is unity for the plane stress case. r_p from Equation (4) in the first iteration is obtained as 13 mm, which is not negligible w.r.t. the crack size of 20 mm. Equation (4), when repeated in an iterative procedure by replacing a by $(a+r_p/2)$ in the new iteration till convergence, shall only increase the value

of r_p from 13 mm. However, the value of r_p of 13 mm from the first iteration itself negates LEFM and supports the existence of the EPFM regime. Refer to Figure 9. Importantly, the actual crack tip plastic zone size as measured from the finite element solution is also of the order of the crack size of 20 mm, which substantiates the EPFM condition near the tip of the crack.

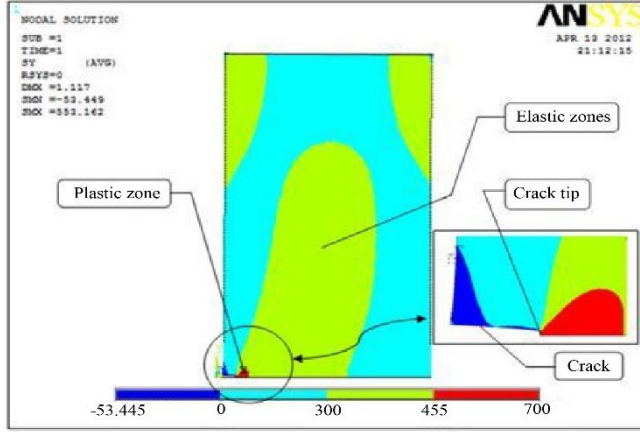


Fig. 9 Crack tip plastic and elastic zones

7. Results and Discussion

The computed final, average value of the J-integral is of the order of 34 N/mm. Refer to Figure 10. HRR value of radial stresses, σ_r , at arbitrarily selected nodes 1-5 in the crack tip plastic zone are theoretically determined from Equation (1) using the stated J integral value and other parameters as discussed previously in Section 3. The selected nodes are chosen slightly away from the crack tip because the HRR solution breaks down at nodes very near the crack tip due to crack tip blunting. The figure illustrates the σ_y stress distribution within the crack tip plastic zone along the y-direction, as obtained from the finite element analysis. The finite element values of σ_r at the selected nodes are presented in Table 1. The values of σ_r are less than σ_y because the tangential stress component, σ_θ , also contributes substantially to deciding the magnitude of σ_y . Refer to Figure 11. The finite element values of σ_r are compared with those obtained from

the theoretical HRR solution. A close agreement among the results affirms the accuracy of the HRR solution.

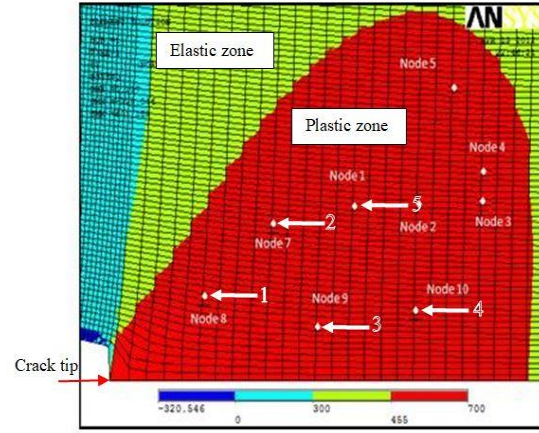


Fig. 10 Finite element stress solution in the y direction and magnified view of crack tip plastic zone and selected nodes in the plastic zone

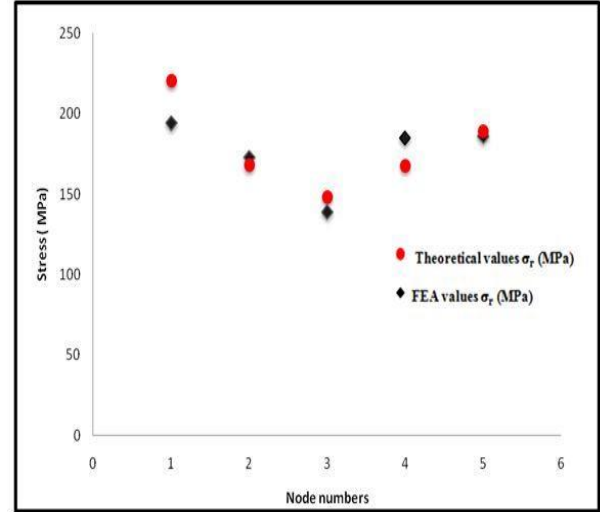


Fig. 11 Comparison between finite element and theoretical HRR values of nodal radial stress, σ_r

Table 1. Comparison between FE and HRR solutions

Node No.	Distance from the crack tip (mm)	Radius r in mm	θ degrees	FE value of σ_r in MPa	Theoretical HRR value of σ_r in MPa	Error %
1	x = 13.37 y = 4.5	14.11	18.67	194.28	220.27	11.8
2	x = 16.20 y = 7.3	17.77	18.7	172.92	168.00	2.9
3	x = 19.17 y = 4.1	19.6	12.08	139.07	148.21	6.2
4	x = 22.74 y = 4.5	23.18	11.2	185.21	167.61	9.5
5	x = 20.1 y = 9.7	22.36	18.5	186.24	189.19	1.6

8. Conclusions and Future Scope

The paper presents finite element validation of the theoretical HRR formulation for the stress distribution around a Mode I crack tip under elastic-plastic fracture conditions existing at the tip. The outcomes of the research lead to the following key conclusions:-

- ANSYS 12 is successfully employed to simulate the elastic-plastic fracture mechanics conditions at the crack tip.
- The J-integral in the vicinity of the crack tip is extracted using a finite element post-processing routine supported by a computer code, and its value is incorporated into the HRR solution.
- Nodal radial stress values in the crack tip plastic zone obtained from finite element analysis are compared with those predicted by the theoretical HRR model, showing good agreement, thereby confirming the validity of the finite element solution.
- Since the authenticity of the HRR solution is well supported in this work by the finite element method with positive results, the researchers can directly and quickly obtain the Mode I crack tip stress solution in EPFM with reasonable accuracy by the finite element method without resorting to the theoretical computations involved in the HRR solution. However, it must be stated here that results from the HRR solution are always more accurate than those obtained from the finite element analysis.
- The present work deals only with nodal radial stresses in the crack tip plastic zone. This procedure can likewise be applied to determine the finite element values of nodal tangential and shear stress in the plastic zone, followed by their comparison with corresponding theoretical HRR solutions.

Acknowledgements

Support received from RVITM, Bangalore, and SVERI's College of Engineering, Pandharpur, during the course of this work is gratefully acknowledged.

References

- [1] Ted L. Anderson, and T.L. Anderson, *Fracture Mechanics Fundamentals and Applications*, 3rd ed., CRC Press, pp. 1-640, 2005. [[CrossRef](#)] [[Google Scholar](#)] [[Publisher Link](#)]
- [2] J.W. Hutchinson, "Singular Behaviour at the End of a Tensile Crack in a Hardening Material," *Journal of the Mechanics and Physics of Solids*, vol. 16, no. 1, pp. 13-31, 1968. [[CrossRef](#)] [[Google Scholar](#)] [[Publisher Link](#)]
- [3] J.R. Rice, and G.F. Rosengren, "Plane Strain Deformation Near a Crack Tip in a Power-Law Hardening Material," *Journal of the Mechanics and Physics of Solids*, vol. 16, no. 1, pp. 1-12, 1968. [[CrossRef](#)] [[Google Scholar](#)] [[Publisher Link](#)]
- [4] J.R. Rice, "A Path Independent Integral and the Approximate Analysis of Strain Concentration by Notches and Cracks," *Journal of Applied Mechanics*, vol. 35, no. 2, pp. 379-386, 1968. [[CrossRef](#)] [[Google Scholar](#)] [[Publisher Link](#)]
- [5] S. Filippi, M. Ciavarella, and P. Lazzarin, "An Approximate, Analytical Approach to the 'HRR'-Solution for Sharp V-Notches," *International Journal of Fracture*, vol. 117, pp. 269-286, 2002. [[CrossRef](#)] [[Google Scholar](#)] [[Publisher Link](#)]
- [6] Junhua Zhao, Wanlin Guo, and Chongmin She, "Three-Parameter Approach for Elastic-Plastic Fracture of the Semi-Elliptical Surface Crack under Tension," *International Journal of Mechanical Sciences*, vol. 50, no. 7, pp. 1168-1182, 2008. [[CrossRef](#)] [[Google Scholar](#)] [[Publisher Link](#)]

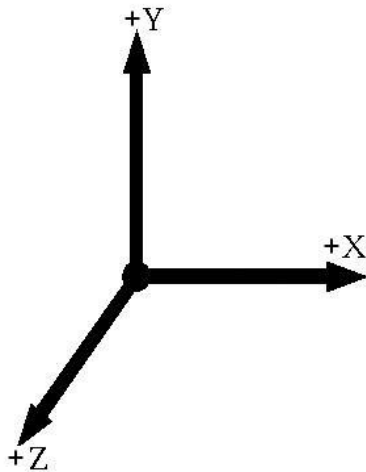
Notations

HRR - Hutchinson, Rice, and Rosengren
 EPFM - Elastic plastic fracture mechanics
 FEA-Finite element analysis
 LEFM-Linear elastic fracture mechanics
 SSY- Small-scale yielding
 LSY - Large-scale yielding
 θ - Angular coordinate of node w.r.t. crack tip
 r - Radial coordinate of node
 σ_{ij} - Stress field tensor
 σ_{YS} - Yield strength
 σ_{UTS} - Ultimate tensile strength
 ϵ_{ij} - Strain field tensor
 ϵ_{YS} - Yield strain
 α - A dimensionless material constant
 n - Work hardening coefficient
 E - Young's modulus
 I_n - HRR integration constant
 $\tilde{\sigma}_{ij}(n, \theta)$ - Dimensionless function of n and θ
 J - J integral
 w - Strain energy density
 u - Displacement vector component
 ds - Length increment along contour
 T_i - Components of the traction vector
 K_I - Mode I stress intensity parameter
 c - Constant (1 for plane stress condition)
 σ_r - Radial stress at node
 σ_θ - Tangential stress at node
 σ_y - Stress in y direction at node
 p - Far field/applied stress
 r_p - Crack tip plastic zone size
 a - Crack length
 $w\#$ - Width of plate
 h - Height of plate
 $f(\alpha\alpha)$ - Configuration factor
 $\alpha\alpha$ - Constant of configuration factor
 n_j - Components of unit vector normal to path
 Γ - Cyclic path

- [7] T. Elguedj, A. Gravouil, and A. Combescure, "Appropriate Extended Functions for X-FEM Simulation of Plastic Fracture Mechanics," *Computer Methods in Applied Mechanics and Engineering*, vol. 195, no. 7-8, pp. 501-515, 2006. [[CrossRef](#)] [[Google Scholar](#)] [[Publisher Link](#)]
- [8] Mahyar S. Dadkhah, and Albert S. Kobayashi, "Further Studies on the hrr Field of a Moving Crack, An Experimental Analysis," *International Journal of Plasticity*, vol. 6, no. 6, pp. 635-650, 1990. [[CrossRef](#)] [[Google Scholar](#)] [[Publisher Link](#)]
- [9] F.P. Chiang et al., "Optical Analysis of HRR Field," *Optical Engineering*, vol. 27, no. 8, pp. 625-629, 1988. [[CrossRef](#)] [[Google Scholar](#)] [[Publisher Link](#)]
- [10] Wei Chen Shi, "On Isotropic Damage Distributions and Evolutions of HRR Field," *Advanced Materials Research*, vol. 139-141, pp. 284-289, 2010. [[CrossRef](#)] [[Google Scholar](#)] [[Publisher Link](#)]
- [11] A. Sotiropoulou, N. Panayotounakou, and D. Panayotounakos, "Analytic Parametric Solutions for the HRR Nonlinear Elastic Field with Low Hardening Exponents," *Acta Mechanica*, vol. 183, pp. 209-230, 2006. [[CrossRef](#)] [[Google Scholar](#)] [[Publisher Link](#)]
- [12] M. Graba, "The Influence of Material Properties and Crack Length on the Q-Stress Value Near the Crack tip for Elastic-Plastic Materials for Centrally Cracked Plate in Tension," *Journal of Theoretical and Applied Mechanics*, vol. 50, pp. 23-46, 2012. [[Google Scholar](#)] [[Publisher Link](#)]
- [13] J. Wang, and C. L. Chow, "HRR Fields for Damaged Materials," *International Journal of Fracture*, vol. 54, pp. 165-183, 1992. [[CrossRef](#)] [[Google Scholar](#)] [[Publisher Link](#)]
- [14] G.B. May, and A.S. Kobayashi, "Plane Stress Stable Crack Growth and J-Integral/HRR Field," *International Journal of Solids and Structures*, vol. 32, no. 6-7, pp. 857-881, 1995. [[CrossRef](#)] [[Google Scholar](#)] [[Publisher Link](#)]
- [15] Wang Zhiqiang, Cai Lixun, and Huang Maobo, "Full Solution for Characterizing Stress Fields Near the Tip Of Mode-I Crack Under Plane and Power-Law Plastic Conditions," *Chinese Journal of Theoretical and Applied Mechanics*, vol. 55, no. 1, pp. 95-112, 2023. [[CrossRef](#)] [[Google Scholar](#)] [[Publisher Link](#)]
- [16] Jianping Xu et al., "A New Prediction Model of Fatigue Crack Expansion Rate Based on HRR Stress Strain Field," *Theoretical and Applied Fracture Mechanics*, vol. 138, 2025. [[CrossRef](#)] [[Google Scholar](#)] [[Publisher Link](#)]
- [17] Mateus B. Neiva, Carlos A. Almeida, and Ivan F.M. Menezes, "Three-Dimensional Numerical Elasto-Plastic Analysis of Stress and Strain Fields Near a Crack Tip," *Theoretical and Applied Fracture Mechanics*, vol. 141, 2026. [[CrossRef](#)] [[Google Scholar](#)] [[Publisher Link](#)]
- [18] Jingxia Yue et al., "Crack Growth in Ni-Cr-Mo-V Steel Using Δ CTOD Elastic-Plastic Model," *Journal of Marine Science and Engineering*, vol. 10, no. 12, pp. 1-15, 2022. [[CrossRef](#)] [[Google Scholar](#)] [[Publisher Link](#)]
- [19] Meiling Xu, Yujin Liu, and Huang Yuan, "Characterization of Crack-Tip Fields for Elastoplastic Fatigue Crack Growth Part I: Analysis of the Δ J-Integral," *Engineering Fracture Mechanics*, vol. 275, 2022. [[CrossRef](#)] [[Google Scholar](#)] [[Publisher Link](#)]
- [20] James G. Malone, Robert Plunkett, and Philip G. Hodge Jr, "An Elastic-Plastic Finite Element Solution for a Cracked Plate," *Finite Elements in Analysis and Design*, vol. 2, no. 4, pp. 389-407, 1986. [[CrossRef](#)] [[Google Scholar](#)] [[Publisher Link](#)]
- [21] M. Kikuchi, "Analysis of HRR Fields of Surface Cracks," *International Journal of Fracture*, vol. 58, pp. 273-283, 1992. [[CrossRef](#)] [[Google Scholar](#)] [[Publisher Link](#)]

Appendix 1

APDL code for obtaining the value of J-integral



ETABLE,ESE,SENE
ETABLE,EVOL,VOLU

```
SEXP,ESED,ESE,EVOL,1,-1
PDEF,ESEDM,ETAB,ESED
PCALC,INTG,T1,ESEDM,YG
PDEF,INTR,SXM,SX
PDEF,INTR,SYM,SY
PDEF,INTR,SXYM,SXY
PVECT,NORM,NX,NY,NZ
PCALC,MULT,VAL1,SXM,NX
PCALC,MULT,VAL2,SXYM,NY
PCALC,MULT,VAL3,SXYM,NX
PCALC,MULT,VAL4,SYM,NY
PCALC,ADD,VAL5,VAL1,VAL2
PCALC,ADD,VAL6,VAL3,VAL4
*GET,DX,PATH,LAST,S
DX=DX/100
PCALC,ADD,XG,XG,,,-DX/2
PDEF,INTR,UX1,UX
PDEF,INTR,UY1,UY
PCALC,ADD,XG,XG,,,-DX
PDEF,INTR,UX2,UX
PDEF,INTR,UY2,UY
```

```
PCALC,ADD,XG,XG,,,,-DX/2
C=(1/DX)
PCALC,ADD,C1,UX2,UX1,C,-C
PCALC,ADD,C2,UY2,UY1,C,-C
PCALC,MULT,VAL7,VAL5,C1
PCALC,MULT,VAL8,VAL6,C2
PCALC,INTG,T2,VAL7,S
PCALC,INTG,T3,VAL8,S
```

```
*GET,JA,PATH,,LAST,T1
*GET,JB, PATH, LAST,T2
*GET, JC, PATH, LAST,T3
JINT=JA-(JB+JC)
JINT2=2*JINT
PDEF, CLEAR
ETABLE, ERAS
PADEL, ALL
```